Perovskite Electrodes for High Temperature Solid Electrolyte Fuel Cells

Yasuo Takeda*, Ryoji Kanno*, Muneyoshi Noda*
and Osamu Yamamoto*

The cathodic polarization of $La_{1-x}Sr_xMO_{3-z}$ (M=Cr, Mn, Fe, Co) electrode sputtered on yttria stabilized zirconia electrolyte was studied at 600–800°C. The study of the exchange current, I_0, as a function of Po_2 and temperature reveals that the rate-determining steps for oxygen reduction are as follows; the charge transfer process for $La_{1-x}Sr_xCoO_{3-z}$, the dissociation of oxygen molecules on the surface for $La_{0.7}Sr_{0.3}FeO_{3-z}$ and $La_{0.7}Sr_{0.3}MnO_{3-z}$, and the oxygen diffusion on the electrode surface for $La_{0.7}Sr_{0.3}CrO_3$. The marked electrode activity of $La_{1-x}Sr_xCoO_{3-z}$ was explained by the high oxygen diffusivity and the high dissociation ability of oxygen molecules.

KEY WORDS: Perovskite oxide/ Solid electrolyte/ Fuel cell/ Oxygen electrode/

I. INTRODUCTION

Solid oxide electrolyte fuel cells (SOFC) have exceptional potential for electric power generation because of the improved kinetics and the availability of high quality by-product heat. However, there are many material problems to be solved to obtain a high performance fuel cell.[1,2] Acceptable O^{2-} ion mobilities occur only above 800–1000°C in the known oxide ion conductors, whose temperature is considerably above the optimum for fuel cell operation. The high operating temperature restricts the freedom of the selection of cell materials. The most significant material limitations at this time are imposed by the cathode and the cathode leads because of the high corrosion effect of oxygen at working temperature. With operating temperature up to 1000°C in air or oxygen atmosphere, the cathode material has to meet the following requirements: high electron conductivity, thermal and chemical stability, sufficient porosity, good adherence at the surface of the electrolyte and the catalitic activity for the oxygen decomposition.[3] Only noble metals or electron conducting metal oxides can be used as the cathode. Noble metals such as platinum must be excluded because of the cost and life (vaporization). Some complex oxides in the perovskite family may satisfy the most of the above requirements. The cell performance of SOFC using the perovskite oxides as the cathode have been extensively reported, which are $PrCoO_3$, $LaFeO_3$, $LaNiO_3$, $LaMnO_3$ and $LaCoO_3$, some of which were used in the form of solid solution with alkaline earth metals in A site to enhance the conductivity.[4–8] However, there are only few reports in which the electrode characteristics of these perovskite materials have been compared systematical-

---

* 武田保雄, 菅野了次, 野田宗良, 山本 治 : Department of Chemistry, Faculty of Engineering, Mie University, Tsu 514, Japan.

ly as high temperature oxygen electrodes on zirconia electrolyte, because of difficulties in separating the effects of morphology. Recently, Isaacs and Olmer[9] have reported the comparison of materials as oxygen catalytic electrodes, where single-point contact electrodes were used to overcome morphology variation. They examined the perovskite-type oxides, $La_{0.5}Sr_{0.5}FeO_3$, $La_{0.8}Ba_{0.2}CoO_3$ and $PrCoO_3$, and reported that $La_{0.5}Sr_{0.5}FeO_3$ showed the highest catalytic activity for oxygen reduction. However, these electrodes are far from the actual scheme, and therefore the total catalytic activity for the real electrode of SOFC are not always reflected in the results.

In this work, the thin films of complex oxides sputtered on yttria stabilized zirconia (YSZ) were studied to determine their effects as oxygen electrodes, because the sputtering method is considered to bring the homogenous films with the relatively good reproducibility. The catalytic activity for oxygen reduction is due to the transition metal ions in B site of perovskite. We chose the series of orthoferrite type perovskite $LaMO_{3-z}$ (M=Cr, Mn, Fe, Co) because of thier large stability at high temperature under oxidation atomosphere.[10] As $LaMO_{3-z}$ (M=Cr, Mn, Fe) show low electric conductiviyt at high temperature, a part of La^{3+} ions were replaced by Sr^{2+} ions in order to enhance the electric conductivity. Two kinds of series of $La_{0.7}Sr_{0.3}MO_{3-z}$ (M=Cr, Mn, Fe and Co; z represents the oxygen deficiency) and $La_{1-x}Sr_xCoO_{3-z}$ ($0 \leq x \leq 0.9$) were studied for their polalization in oxygen reduction.

2. EXPERIMENTAL

Yttria-doped (8 mole%) zirconia was used as electrolytes. The mechanically mixed powder of Y_2O_3 (99.99% purity) and zirconia (chemicla grade) was calcined at 1000°C, then ground and pressed into pellets (12 mm diam. ×2 mm hight) under a pressure of 2,000 kg/cm², and sintered at 1500°C for 3 hr. The density thus obtained was greater than 95% of theoretical value. Porous platinum was used as the counter electrode, which was prepared by painting platinum past (Englehard 6080), and firing it at 1000°C in open air for 3 hr. The platinum electrode was divided into two parts; one part was used as the reference electrode (Fig. 1). The perovskite-type oxides $La_{1-x}Sr_xMO_3$ (M=Cr, Mn, Fe, Co) were obtained from $La(OH)_3$ (chemical grade), $SrCO_3$ (chemical grade), and the corresponding oxides or carbonate, Cr_2O_3, $MnCO_3$, Fe_2O_3 and Co_3O_4 (chemical grade). The mixtures of the starting materials were ground and fired in open air at 1300°C for 15 hr.

A ULVAC-1104 sputtering system was used for the electrode film deposition. The powdered $La_{1-x}SrM_xO_{3-z}$ target was used as the cathode. The $La_{1-x}Sr_xMO_{3-z}$ films were RF sputtered onto the tablet of YSZ in an argon pressure of 1×10^{-2} torr. The RF power was 200W ($\simeq 2.5$ W/cm²). Film thickness was calculated from the weight gain and the theoretical density of the oxides, which was in good agreement with that estimated from SEM pictures. The deposition rate was around 0.5 μm/hr. As-sputtered film was amorphous under the observation of x-ray diffraction. The obtained films were annealed at 800°C for 2 hr in order to crystallize to perovskite structure. The X-ray diffraction patterns of the annealed $La_{1-x}Sr_xMO_{3-z}$ films showed only the lines due to the corresponding perovskite structure. The atomic
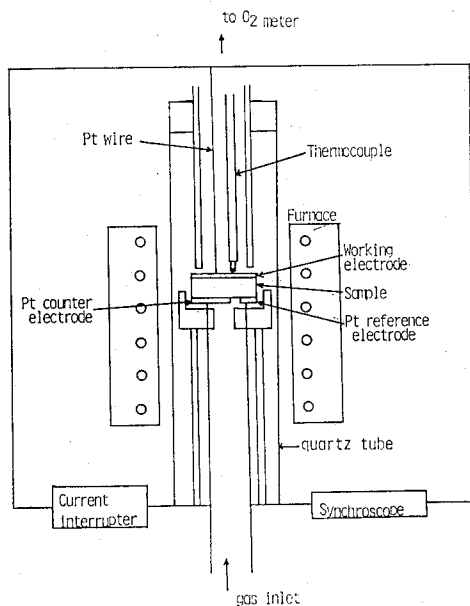
Fig. 1. Experimental cell.

ratios of cations measured by dispersive x-ray analysis in a scanning electron micro-scope were in agreement with those of the target.

The electrical conductivity of the film was measured in open air by the four-terminal method using direct current over a temperature range from room tempera-ture to 900°C. The cathodic overpotential for the electrodes sputtered on YSZ was measured by the current-interruption tehcnique to remove the IR-drop contribution. The schematic system is shown in Fig. 1. The steady-state residual voltage (overpo-tential) between the test and reference electrodes was measured under a constant current drain. The polarization experiments were carried out up to 800°C to avoid the progress of the reaction with YSZ electrolyte.

3. RESULTS AND DISCUSSION

3-1) Electrical conductivity of sputtered electrode

The resistivities of the SOFC system consist of the cell components of the elec-trolyte, interconnection materials, cathode materials, and anode materials. Fee et al.[2] estimated the resistivities of each cell component based on the useful generator design rproposed by Westinghouse Electric corporation.[11] The relatively high resis-tivity of the electolyte and interconnection does not impact too significantly on cell performance because of the short current flow paths in these materials. As a result of high resistivity from the long current path, the cathode is principal contributor to voltage losses due to the internal resistance in SOFC. Therefore, the most important requirement for the cathode material is to have the high electrical conductivity. In Fig. 2, the electrical conductivities of the sputtered films of $La_{1-x}Sr_xMO_{3-z}$ are shown as a function of temperature. The thickness of the films is around $2\,\mu m$. The

Y. Takeda, R. Kanno, M. Noda and O. Yamamoto
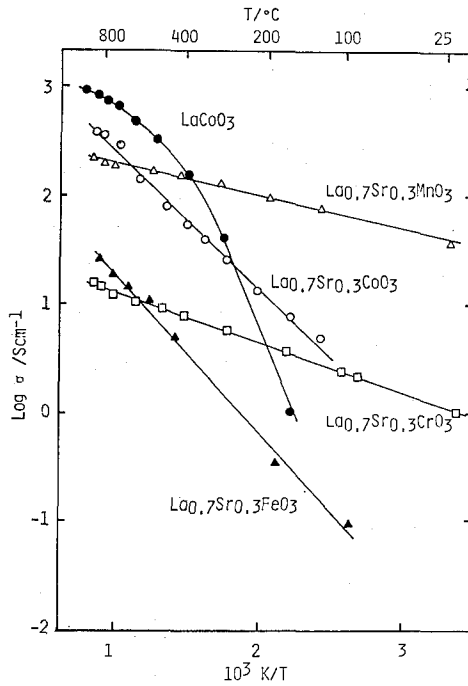
Fig. 2. Temperature dependence of the electrical conduct
ivity of the sputtered films of $La_{1-x}Sr_xMO_{3-z}$.

conductivities of these films are of the order of 10^1–10^3 Scm^{-1}, and shows semiconcud-
tive behavior in the temperature range measured. These values are fairly well
coincide with the reported values measured for sintered samples. The detailed dis-
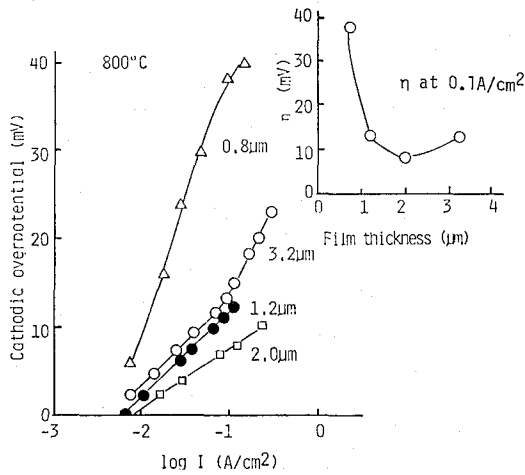cussions have already been presented.[12]

Fig. 3. Cathodic polarization curves at 800°C for the
sputtered $LaCoO_{3-z}$ electrodes with various
thickness.

3–2) Cathodic polarization of sputtered electrodes

The cathodic polarizations at 800°C for sputtered perovskite oxide electrodes were measured for the various electrode thickness. In Fig. 3 are shown, as an example, the ovrepotential vs. current density curves at 800°C for the sputtered La-CoO$_{3-z}$ electrodes. The relation between the thickness and the ovrepotential at 0.1 A/cm^2 is also shown in Fig. 3. A minimum overpotential is observed for the electrode with around 2 μm thickness. Similarly, all electrodes showed the lowest polarization at the electrode thickness of around 2–3 μm. From the SEM observation of the electrode surface having various thickness, it appeared that: the electrode with around 2 μm thickness has a large number of pores of 1 μm diameter in average, which looks like the ideal porous gas electrode; cracks and separations from the electrode surface occur in the thicker electrode with 3 μm or more; and the irregular form of pores
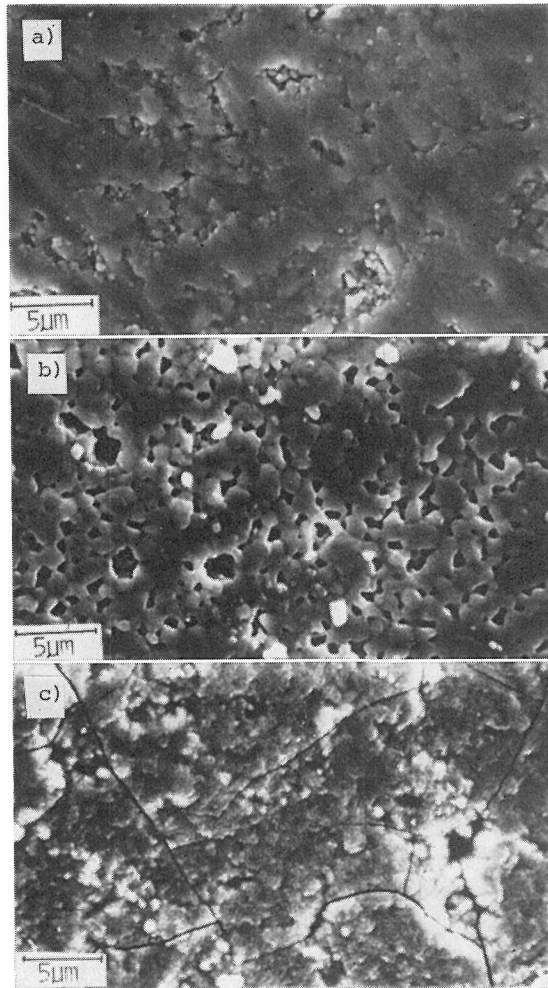

Fig. 4. SEM photographs of the sputtered LaCoO$_{3-z}$ films.
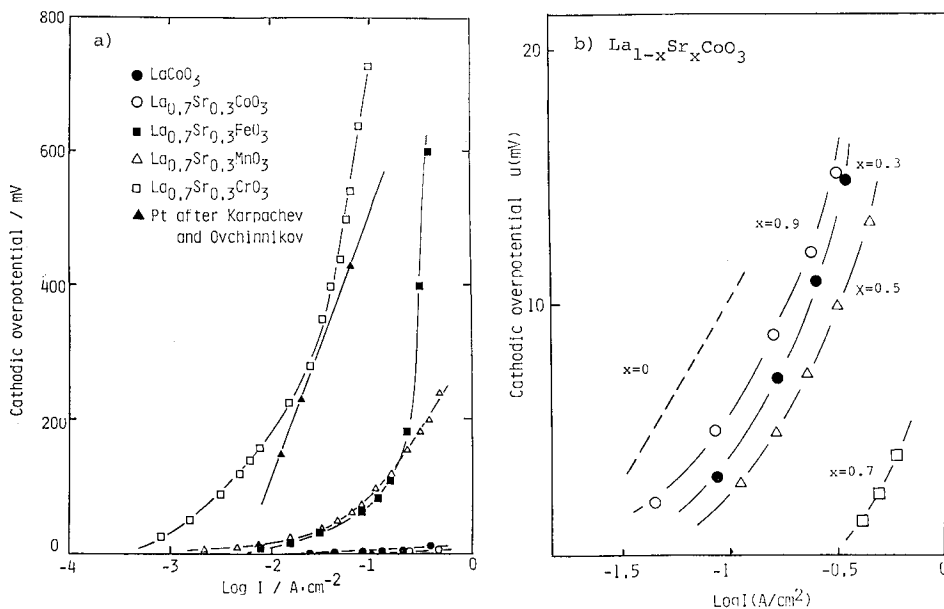The film thickness: a) 0.8 μm, b) 2.0 μm, c) 3.2 μm.

Fig. 5.   Cathodic polarization curves at 800°C for the sputtered $La_{1-x}Sr_xMO_{3-z}$ electrodes.
a) $La_{0.7}Sr_{0.3}MO_{3-z}$(M=Cr, Mn, Fe, Co) and $LaCoO_{3-z}$
b) $La_{1-x}Sr_xCoO_{3-z}$.

are seen in places for the thinner electrode of about 1 μm thickness.   The $LaCoO_{3-z}$ surfaces of SEM observation for various thickness are shown as an example in Fig. 4. The dependency of the cathodic polarization on the electrode thickness is strongly related to the electrode porosity.

In Fig. 5, cathodic polarization curves at 800°C in open air are shown for the electrodes of $La_{0.7}Sr_{0.3}MO_{3-z}$ (M=Cr, Mn, Fe, Co) and $La_{1-x}Sr_xCoO_{3-z}$ ($0 \leq x \leq 0.9$), where the curves showing a minimum polarization overpotential are represented (around 2 μm–3 μm) in thickness).   The curve of porous Pt electrode at 800°C reported by Karpachev and Ovchnnikov[13] is also shown.   The perovskite electrodes except for $La_{0.7}Sr_{0.3}CrO_{3-z}$ show by far lower overpotential for oxygen reduction than porous Pt electrode.   Especially, the series of Co-perovskite $La_{1-x}Sr_xCoO_{3-z}$ shosw extremely low overpotential.   The electrode with x=0.7 scarcely caused the polarization even at a high current density of 1 A/cm². $La_{1-x}Sr_xMnO_3$[14] and $La_{1-x}Sr_xCoO_3$ (x=0, 0.3)[15] electrodes prepared by plasuma-splay method on the Westinghous Co. style electrolyte have been reploted to have the cathodic overpotential of 100–150 mV at 0.5 A/cm² and more than 200 mV at 0.3 A/cm² at 1000°C, respectively.   Direct comparison with our data from the sputtered electrodes is difficult because the both cell scheme are largely different and, in addition, their electrodes have possibly chemically reacted with the electrolyte (YSZ) at the operating temperature of 1000°C. Our preliminary study indicated that the chemical reaction of perovskite electrode and YSZ electrolyte occurred at more than 1000°C producing $La_2Zr_2O_7$ or Sr_2ZrO_4[12] and the decline of the electrode performance was observed at that measuring temperature.

3–3)   Reaction mechanisms of $La_{1-x}Sr_xMO_{3-z}$ (M=Cr, Mn, Fe, Co)

When an overpotential, η, is applied across the electrode-electrolyte interface, the current I is expressed as a well-known Butler-Volmer equation,

$$I = I_0 \left[-\exp(\alpha_a nF\ \eta/RT) + \exp(\alpha_c nF\ \eta/RT)\right] \qquad [1]$$

where α_a and α_c are the anodic and cathodic transfer coefficients, respectively. At low overpotential ($\eta \ll RT/F$), ohmic behavior,

$$\eta = (RT/I_0F)\ I \qquad [2]$$

is obtained. Where RT/I_0F is called as a polarization resistance. Exchange current density I_0 reflects the kinetic properties of the interfacial system, so we can estimate the mechanisms of electrode reactions by measuring the dependencies on the temperature and partial oxygen pressure.[16-18] To know I_0 from equation [2], the over potential η must be measured in the region where η is linear with the applied current I. At 600°C, η must be $\ll RT/F = 8.314 \times 873/96500 = 75$ mV. As shown in Fig. 6, η showed a linear relation with I below $\eta = 25$ mV. We measured the electrode overpotential η as a function of current I for $\eta < RT/F$ at 600–800°C under the oxygen pressure of $Po_2 = 0.5$–10^{-2} atom. The exchange current density I_0 was calculated from the polarization resistance RT/I_2F and plotted against the temperature and oxygen partial pressure.

In Figs. 7 and 8, the temperature and Po_2 dependence of I_0 of $LaCoO_{3-z}$ electrode are shown as a set of isobaric plots of log I_0 vs. $1/T$ and isotherm plots of Log I_0 vs. Log Po_2, respectively. In Fig. 7, each of the curves gives the same activation energy (230 kJ/mol), which implies that at each temperature I_0 has the same Po_2 dependence. The plots in Fig. 8 show that I_0 has a $Po_2^{1/4}$ dependence at each temperature.

The I_0 data plotted as isotherms as a function of log Po_2 for the perovskite elec-
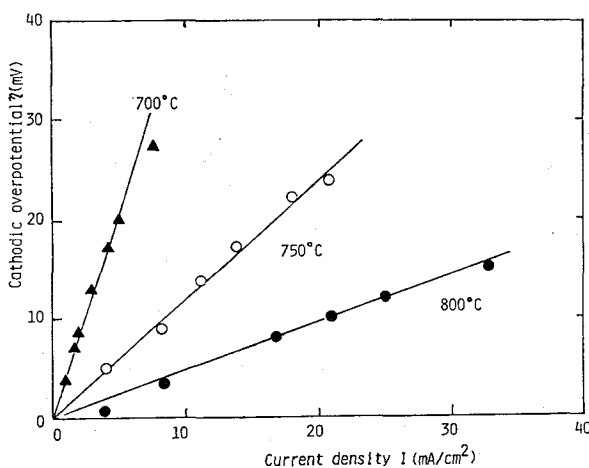

Fig. 6.   Plots of cathodic overpotential η vs. current I at low overpotential for the sputtered $LaCoO_{3-z}$ electrode at various temperature.
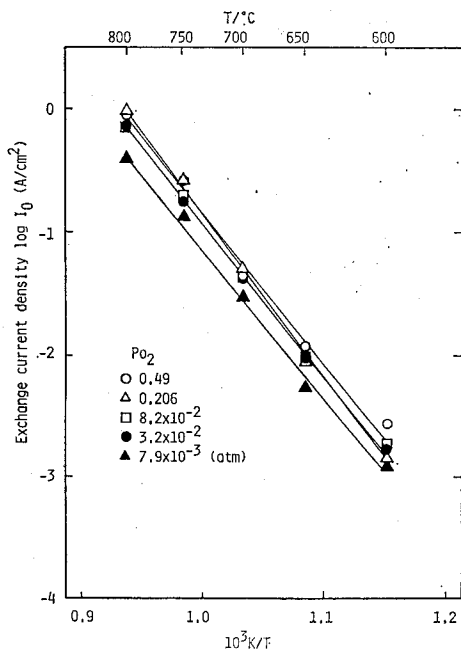
Fig. 7. Temperature dependence of the exchange currtne density for the $LaCoO_{3-z}$ electrode under various oxygen partial pressures.
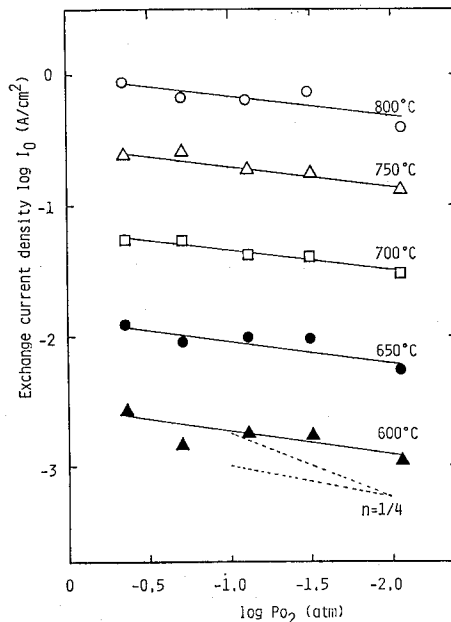

Fig. 8. Oxygen partial pressure dependence of the exchange current density for the $LaCoO_{3-z}$ electrode at various temperature.
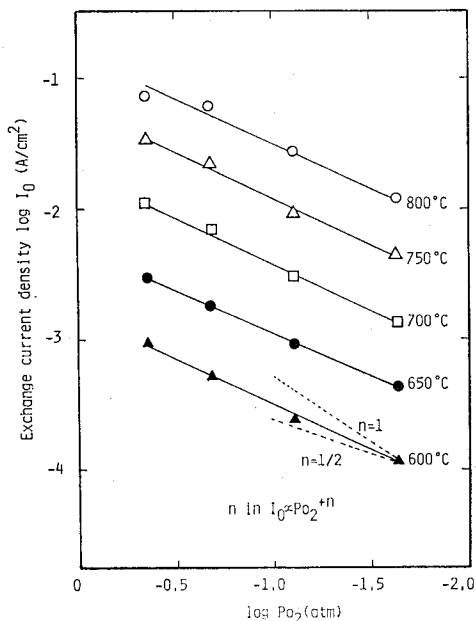

Fig. 9. Oxygen partial pressure dependence of the exchange current density for the $La_{0.7}Sr_{0.3}FeO_{3-x}$ electrode at various temperatures.

Fig. 10. Oxygen partial pressure dependence of the exchange current density for the $La_{0.7}Sr_{0.3}MnO_{3-z}$ electrode at various temperatures.

Fig. 11. Oxygen partial pressure dependence of the exchange current density for the $La_{0.7}Sr_{0.}CrO_{3-z}$ electrode at various temperature.

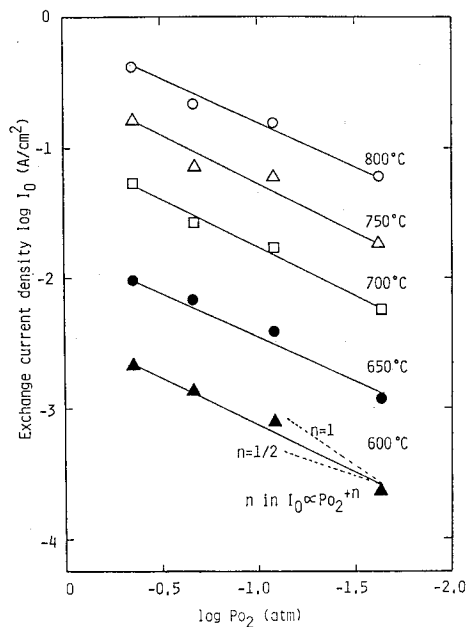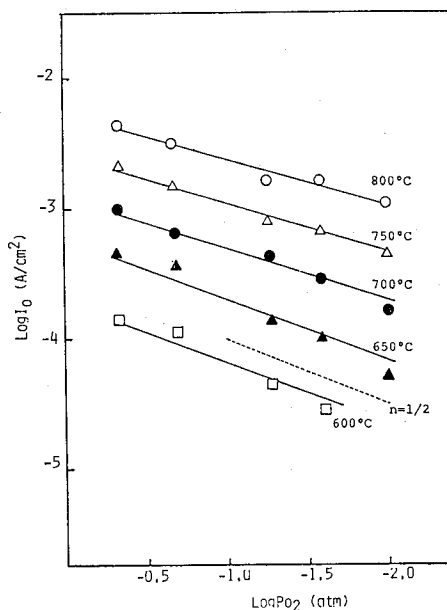Table I Po_2 dependency and activation energy for $La_{1-x}Sr_xMO_{3-z}$ electrode

electrode	n in $I_0 \propto Po_2^n$	activation energy (kJ/mol)
$La_{0.7}Sr_{0.3}CrO_{3-z}$	1/2	130
$La_{0.7}Sr_{0.3}MnO_{3-z}$	3/4	180
$La_{0.7}Sr_{0.3}FeO_{3-z}$	3/4	160
$LaCoO_{3-z}$	1/4	230
$La_{0.7}Sr_{0.3}CoO_{3-z}$	1/4	220
$La_{0.5}Sr_{0.5}CoO_{3-z}$	1/4	220
$La_{0.3}Sr_{0.7}CoO_{3-z}$	1/4	220

trodes, $La_{0.7}Sr_{0.3}CrO_{3-z}$, $La_{0.7}Sr_{0.3}MnO_{3-z}$ and $La_{0.7}Sr_{0.3}FeO_{3-z}$ are also shown in Figs. 9, 10 and 11. I_0 for $La_{0.7}Sr_{0.3}CrO_{3-z}$ shows $Po_2^{1/2}$ dependency and for $La_{0.7}Sr_{0.3}MnO_{3-z}$ and $La_{0.7}Sr_{0.3}FeO_{3-z}$, $Po_2^{3/4}$ dependency. In Table I, the Po_2 dependency and the activation energy for each perovskite electrode are listed. The value of n in the form of $I_0 \propto Po_2^n$ is characteristic for the metal ions in B site in perovskite. $n=1/4$ for Co, 3/4 for Fe and Mn and 1/2 for Cr.

The overall reaction at oxygen electrode is

$$O_2(g) + 4e' + 2V_0^{\cdot\cdot} \longrightarrow 2O_0^\times \qquad [3]$$
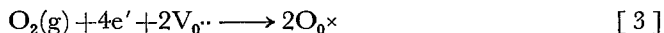
where $V_0^{\cdot\cdot}$ and $O_0^\times$ refer, respectively, to vacancies and oxygen ions in the electrolyte. In the case of perovskite oxide electrode, the reaction [3] may consist of the following
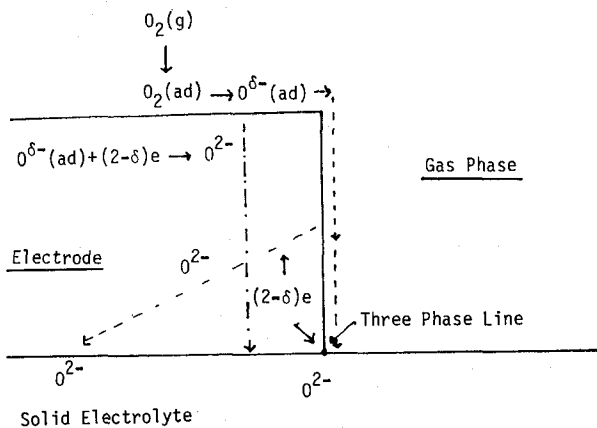
$$O_2(g)$$
$$\downarrow$$
$$O_2(ad) \rightarrow O^{\delta-}(ad) \rightarrow,$$

$$O^{\delta-}(ad)+(2-\delta)e \rightarrow O^{2-}$$

Gas Phase

Electrode O^{2-}

$(2-\delta)e$

Three Phase Line

O^{2-} O^{2-}

Solid Electrolyte

Fig. 12. Reaction steps for the perovskite oxide electrode.

Table II Elementary reaction steps and the value of n, characteristic of rate determining step

	elementary reaction	n in $I_0 \propto Po_2{}^n$
I	$O_2(g) \rightarrow O_2(ad)$	1
II	$O_2(ad) \rightarrow 2O(ad)$	1–0
III	$O(ad)+2e \rightarrow O^{2-}$	1/4
IV	surface diffusion	1/2

processes: (I) gaseous diffusion to the electrode surface, (II) dissociation and physical adsorption on the electrode, (III) charge transfer at the surface and/or inside of the electrode, (IV) surface and/or bulk diffusion of oxide ions to the electrolyte. The schematic process is illustrated in Fig. 12.

For the Pt electrodes, numerous works have been continued and the detailed electrode reactions have been discussed.[15-19] I_0 is a measure of the rate of ovreall electrode reaction and the dependency on Po_2 has been revealed to reflect the earch rate determining step. In Table II, the value of n in $I_0 \propto Po_2{}^n$ are given with corresponding rate-determining steps based on the consideration of Pt electrode. As these relation are led from the various assumption and, in addition, are for the metal electrode such as platinum, it may be problem to apply these relation fully to the oxide electrodes. But all the electrode reactions are essentially constructed by the adsorption, dissociation, diffusion and charge transfer, so the relations in Table II can be roughly applicable to the perovskite electrode.

In the case of $La_{1-x}Sr_xCoO_{3-z}$ electrode, I_0 is proportional to $Po_2{}^{1/4}$. From Table II, the rate-determining step is considered to be the charge transfer process. In the metal electrode such as platinum, adsorbed and dissociated oxygens mainly diffuse to the three-phase contact area and dissolve to the electrolyte with charge transfer process ($O_{ad}+2e \rightarrow O^{2-}$) which acrossing the electrode/electrolyte phase boundary. It is characteristics for Pt electrode that most part of reaction occurs at the

three-phase contact area. In the oxide electrode, especially containing the transition metals in the composition, the charge transfer process possibly occurs in every sites where transition metal ions grow their d-orbitals. The dissociated O atom physisorped on the electrode surface will soon transfer to chemisorption state, that is,

$$O_{ad} + \delta e \rightarrow O_{ad}{}^{\delta-} . \qquad [4]$$

During the diffusion through the surface and/or in the bulk, O_{ad} atoms combine with electrons to form O^{2-} ions. The charge transfer process,

$$2(O_{ad} + 2e' + V_0{}^{\cdot\cdot}) \rightarrow 2(O_0{}^{\times} + V_{ad}) \qquad [5]$$

does not necessarily proceed with one step, although we cannot distinguish the each step. Wang and Nowick[10] calculated the activation energy of the Pt electrode to be 0.99eV (about 100 kJ/mol) under the charge transfer process. The value of $LaCoO_{3-z}$ electrode (230 kJ/mol) is tiwce as large as that of Pt electrode. Nevertheless, Co-perovskite electrode can hold extremely large current flow under the low polarization compare to Pt electrode (Fig. 3). This means that the effectual reaction surface is very large in $La_{1-x}Sr_xCoO_{3-z}$ electrode, that is, charge transfer occurs at every places such as on the surface, in the bulk, at the electrode-electrolyte interface etc. As the rate-determining step is charge transfer process, the rates of adsorption, dissociation and diffusion are faster than that of charge transfer process. In general, perovskite oxides having oxygen vacancy show the high oxide on conductivity. The chemical diffusion coefficient of $LaCoO_3$ measured by chemical relaxation method[20] shows high value such as $\tilde{D} = 5 \times 10^{-6} \, cm^2 s^{-1}$ at 800°C. At the surface, the diffusion increases in few figures comparing to the bulk diffusion. As shown in Figs. 3 and 4, low polarization is realized for the electrode having large amount of pores. The surface diffusion is considered to be important than the bulk diffusion for the oxygen reduction process in electrode. Moreover, $La_{1-x}Sr_xCoO_{3-z}$ series have been known as an excellent catalysis for oxidation-reduction process.[21] The superior activity of Co-perovskite electrode is explained by these high oxygen diffusion coefficient and high catalytic activity for the gas decomposition.

In the $La_{0.7}Sr_{0.3}FeO_{3-z}$ and $La_{0.7}Sr_{0.3}MnO_{3-z}$ electrodes, I_0 is proportional to $Po_2{}^{3/4}$. The rate-determining step is considered to be the dissociation of adsorbed oxygen molecules to oxygen atom. $La_{1-x}Sr_xMO_{3-z}$ (M=Mn, Fe) has high oxide ion conductivity[20] same as $La_{1-x}Sr_xCoO_{3-z}$ and also are expected to have wide area of effective reaction surface. Nevertheless, the activity for the electrode is largely inferior to that of $La_{1-x}Sr_xCoO_{3-z}$. This may be due to the difference of catalytic ability for the oxygen gas decomposition. For the perovskite system of $La_{1-x}Sr_xMO_{3-z}$ (M=Co, Fe, Mn), the activation energies of I_0-T curve did not depend on the partial oxygen pressure. Normally, the content of oxygen vacancy, z, in the perovskite oxides depends on the oxygen partial pressure at high temperature. The results above show that the oxygen diffusion process is not the rate determining step for the Co, Fe and Mn perovskite electrode.

The I_0 in $La_{0.7}Sr_{0.3}CrO_{3-z}$ electrode showed the $Po_2^{1/2}$ dependence (Fig. 11). From Wang and Nowik consideration,[16] the rate determining step is considered to be the surface diffusion of oxygen atom or oxide ion. The diffusion coefficient of oxide ion in $La_{1-x}Sr_xCrO_{3-z}$ system has not been yet measured. Mizusaki et al.[22] have studied the non-stoichiometry of $La_{1-x}Sr_xCrO_{3-z}$ (x=0.1–0.3) at high temperature under various oyxgen pressure. They reported that for $La_{0.7}Sr_{0.3}CrO_{3-z}$ the composition is perfectly stoichiometric, that is, $La_{0.7}Sr_{0.3}CrO_{3.0}$ under the condition of $Po_2 > 10^{-4}$ atom at 800–1000°C. The oxygen diffusion rate in $La_{0.7}Sr_{0.3}CrO_3$ must be very slow due to their stoichiometric composition. The charge transfer reaction at the electrode surface does not proceed because of the low oxygen diffusion. Therefore the reaction occurs only at the three-phase contact areas same as the case of Pt electrode. This may be due to the low electrode activity of $La_{0.7}Sr_{0.3}CrO_3$ electrode.

4. SUMMARY

The $La_{1-x}Sr_xCoO_{3-z}$ electrode shows excellent electrode activity although the ability of charge transfer per unit is lower than Pt. The high activity comes from the large effective surface area for the reaction due to the high oxygen diffusion and high catalytic activity. In $La_{1-x}Sr_xMO_{3-z}$ (M=Fe, Mn), the ability of adsorption and dissociation is considered to be lower than the $La_{1-x}Sr_xCoO_{3-z}$ electrode. The low activity of $La_{1-x}Sr_xCrO_{3-z}$ electrode is caused by the low diffusivity of oxygen.

Kojima et al.[23] calculated the bulk and surface electronic structures of perovskite oxides such as $LaCoO_3$, $LaFeO_3$ and $LaAlO_3$ by DV-Xα cluster method and showed only the $LaCoO_3$ exhibited a rather high electron density of state near the Fermi level. The marked catalysis by $LaCoO_3$ is associated with electron occupation of crystal field d state near E_F and with the buildup of surface charge so as to enhance the electron transfer between a surface cation and an interacting molecule. The difference in activity of oxygen reduction between $La_{1-x}Sr_xCoO_{3-z}$ and other perovskite is actually due to the difference of the catalytic ability. Perovskite oxide, $La_{1-x}Sr_xCoO_{3-z}$, is marked electrode material for SOFC owing to their high oxygen diffusivity and the dissociation ability for the molecule.

REFERENCES

(1) A.O. Isenberg, National Fuel Cell Seminar Abstracts, Newport Beach, California, Nov. 14–18, 1982, pp. 154–156
(2) D.C. Fee, S.A. Zwick, and J.P. Ackerman, Proceedings of the conference on high temperature solid oxide elecrolyes, Upton, New Yorks, 1983, pp. 27–36
(3) F.J. Rohr, "Solid Electrolyte", P. Hagenmuller and W. van Gool, Editors, p. 431, Academic Press, New York (1978)
(4) D.W. White, General Electric Res. and Develop, Rep. No. 68-c-254 (1978)
(5) R. Steiner, F.J. Rohr, and W. Fischer, Proc. Int. Symp. Fuel Cells, 4th, Antwerpen 114, (1972)
(6) F.J. Rohr, Proc. EUCHEM-conf. Elman, W. Germany, (1975)
(7) C.S. Tedmon, Jr., H.S. Spacil and S.P. Mitoff, *J. Electrochem. Soc.* **116**, 1170 (1969)
(8) Y. Ohno, S. Nagata, and H. Sato, *Solid State Ionics* **3/4**, 439 (1981)
(9) H.S. Isaacs and L.J. Olmer, *J. Electrochem. Soc.* **129**, 436 (1982)

(10) T. Nakamura, G. Petzow and L.J. Guchler, *Mat. Res. Bull.* **14**, 649 (1973).
(11) Westinghouse Electric Corporation, "Thin Film Battery Fuel Cell Power Generating System," 5th Quarterly Report, pp. 24 (1979).
(12) O. Yamamoto, Y. Takeda, R. Kanno and M. Noda, Solid State Ionics, in press.
(13) S.V. Karpachev and Yu. Ovchinnikov, *Sov. Electrochem.* **5**, 200 (1969).
(14) F.J. Rohr, "Applications of Solid Electrolyte", T. Takahashi and A. Kozawa Ed. p196 (1980).
(15) Y. Ohno, S. Nagata and H. Sato, *Solid State Ionics*, **9 & 10**, 1001 (1983).
(16) Da. Yu. Wang and A.S. Nowich, *J. Electrochem. Soc.*, **126**, 1155 (1979).
(17) T.H. Etsell and S.N. Flengas, *J. Electrochem. Soc.*, **118**, 1890 (1971).
(18) J. Sasaki, J. Mizusaki, S. Yamauchi and K. Fueki, *Bull. Chem. Soc. Japan*, **54**, 1688 (1981).
(19) J. Fouletier, P. Fabry and M. Kleitz, *J. Electrochem. Soc.*, **123**, 204 (1976).
(20) T. Ishigaki, S. Yamauchi, J. Mizusaki, K. Fueki and H. Yamura, *J. Solid State Chem.*, **54**, 100 (1984).
(21) R.J.H. Voorhoeve, J.P. Remeika and L.E. Trimble, *Annals of the New York Academy of Sciences*, **272**, 3 (1976).
(22) J. Mizusaki, S. Yamauchi, K. Fueki and A. Ishikawa, *Solid State Ionics*. **12**, 119 (1984).
(23) I. Kojima, H. Adachi and I. Yasumori, *Surface Science*, **130**, 50 (1983).